TECHNICAL NOTES 7

AUTOGENOUS MEDIA SEPARATORS

Autogenous Media Separators

Manufactured dense media usually consist of a suspension of heavy particles that are sufficiently fine to remain in uniform suspension under the force field (gravity or centrifugal) that prevails in the separating unit. The particles to be separated can move more or less independently of each other and are free to float or sink depending on their density relative to the apparent density of the medium suspension. Although particle-particle interactions are significant in a manufactured medium separator, they are usually neither sufficiently frequent nor intense to significantly influence the cut point that is achieved in the separator. However, particle-particle interactions can have a significant influence on the separating efficiency that is actually achieved in the equipment. In an autogenous medium separator, particle-particle interactions are significant and dominant since it is the close interactions between the particles that generate the dense environment in which particles can separate.

The primary phenomenon that occurs is an autogenous medium separator is stratification in the dense bed of particles. Whenever a bed of particles is disturbed and is allowed to settle, the particles will exhibit some tendency to stratify. The heavier particles will tend to find their way to the bottom of the bed and the lighter particles will tend to migrate to the top of the bed. Autogenous media separators rely on stratification of the bed to effect a separation and they are designed to promote rapid and effective stratification of the particle bed.

The stratification behavior of a particle bed can be described in terms of the potential energy of all the particles in the bed. Stratification acts to minimize the total potential energy of the bed by rearrangement of the particles in the bed. This principle was used by Mayer to provide a quantitative description of the behavior of separation equipment such as the jig. However, a consideration of potential energy alone does not provide an adequate description of the actual stratification process as it occurs in practical operations. No matter how effective the stratifying action of the machine is, perfect stratification is never possible. A multitude of random processes influence the behavior of each particle during the time that it passes through the stratification zone of the equipment and these combine to destroy the ideal stratification pattern that is predicted by potential energy considerations alone. The ideal stratification pattern tends to create sharply defined layers in the bed. Sharp boundaries between layers cannot be maintained in the face of the variety of random perturbations that are felt by the particles. The sharp boundaries consequently become diffuse by a diffusion type mechanism which always acts to oppose the ideal stratification pattern.
Lovell *et. al.* in Leonard J W Ed Coal Preparation 5th edition p 350 give a colorful graphic description of the relationship between the pulsation of the jig bed and the motion of the particles as can be sensed by inserting the hand into the bed. "At the peak of the pulsion stroke, the particles must be free to move relative to each other and during the suction stroke they should be firmly held by the suction of the bed." It is this combination of relative motion of the particles and the holding action of the bed during the suction stroke that produces a stable stratification profile that can be split at the end of the jig chamber to produce the desired products.

7.1 A Quantitative model for stratification

A useful model for stratification that is successful in describing the behavior of operating industrial

equipment can be developed by considering the interaction of the potential energy profile that drives the stratification process together with the random diffusion process that tends to break down the ideal stratification profile.

The variation of potential energy when two particles of different density interchange positions in a settled bed is the driving force for stratification. Consider an isolated particle of density ρ in a bed of particles all having density $\bar{\rho}$. The change in potential energy when the isolated particle changes position with a particle at the average density can be calculated as shown in Figure 7.1.

$$\begin{aligned}\Delta E &= E(\text{particle at } H + \Delta H) - E(\text{particle at } H) \\ &= v_p\rho(H + \Delta H)g + v_p\bar{\rho}H - v_p\bar{\rho}(H + \Delta H)g - v_p\rho Hg \\ &= v_p g(\rho - \bar{\rho})\Delta H\end{aligned} \tag{7-1}$$

The rate of change of potential energy as the particle of density ρ increases its height in a bed of average density $\bar{\rho}$ is therefore given by

$$\frac{dE}{dH} = v_p g(\rho - \bar{\rho}) \tag{7-2}$$

This potential energy gradient causes the particle of density ρ to migrate upward or downward depending on the sign of $\rho - \bar{\rho}$. If $\rho > \bar{\rho}$ the particle will move down and *vice versa.* The rate at which particles move relative to the bed is proportional to the energy gradient and the migration velocity is given by $u\frac{dE}{dH}$. u is called the specific mobility of the particle and is defined as the velocity at which a particle penetrates the bed under a unit potential energy gradient. u is a strong function of particle size and shape and the bed expansion mechanism but is independent of the particle density. The flux of particles of density ρ in a bed of average density $\bar{\rho}$ caused by the potential energy gradient is given by

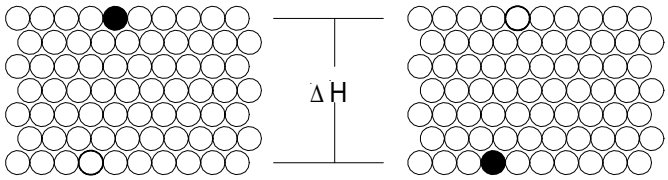

Figure 7-1 *Change of potential energy when a heavy particle changes position in a bed of particles.*

$$n_s = -C_\rho u\frac{dE}{dH} \qquad \text{m}^3/\text{m}^2\,\text{s} \tag{7-3}$$

C_ρ is the concentration of particles of density ρ in the bed expressed as the solid volume fraction. The negative sign reflects the fact that each particle will tend to move down the potential energy gradient so as to ultimately minimize the total potential energy in accordance with Mayer's principle. n_s is called the stratification flux. Combination of equations (7.2) and (7.3) gives

$$n_s = -C_\rho u v_p g(\rho - \bar{\rho}) \tag{7-4}$$

Opposing the stratification flux is the diffusive flux due to the random particle-particle and particle-fluid interactions within the bed. This flux is described by a Fickian equation of the type

$$n_D = -D\frac{dC_\rho}{dH} \tag{7-5}$$

The diffusion coefficient D is dependent on the particle size, shape and bed expansion mechanism. A dynamic state of stratification equilibrium exists in the bed when the tendency of the particles to stratify under the influence of the potential energy gradient is exactly balanced by tendency to disperse under the influence of the concentration gradient that is created by the stratification action. This dynamic equilibrium is defined by

$$n_D = -n_s \tag{7-6}$$

so that

$$\frac{dC_\rho}{dH} = -\frac{ugv_pC_\rho}{D}(\rho - \bar{\rho}) \tag{7-7}$$

This can be written in terms of the relative height $h = \frac{H}{H_b}$, where H_b is the total bed depth and the specific stratification constant

$$\alpha = \frac{ugv_pH_b}{D} \qquad \text{m}^3/\text{kg} \tag{7-8}$$

$$\frac{dC_\rho}{dh} = -\alpha C_\rho(\rho - \bar{\rho}(h)) \tag{7-9}$$

α is independent of particle density but will be a strong function of particle size and bed expansion mechanism. The average bed density is a function of h as indicated in equation (7.9) and is given by

$$\bar{\rho}(h) = \int_0^\infty \rho C_\rho(h)\, d\rho \tag{7-10}$$

A solution to equation (7.9) gives the vertical concentration profile of particles of density ρ. No boundary conditions can be specified *a priori* for equation (7.9) because it is not possible to specify the concentration of any particle type at either the top or bottom or at any intermediate level in the bed.

However, the solution to equation (7.9) must satisfy the conditions

$$\int_0^1 C_\rho dh = C_\rho^f \qquad \text{for all } \rho \tag{7-11}$$

where C_ρ^f is the concentration of particles of density ρ in the feed to the bed and

$$\int_0^\infty C_\rho d\rho = 1 \qquad \text{for } 0 \le h \le 1 \tag{7-12}$$

In practice the particle population is discretized into n grade classes each of which has a unique

density and equation (7.9) - (7.12) are written in discrete form

$$\frac{dC_i(h)}{dh} = -\alpha C_i(h)(\rho_i - \bar{\rho}(h)) \qquad \text{for } i = 1,\ 2,\ .....n \tag{7-13}$$

with

$$\bar{\rho}(h) = \sum_{i=1}^{n} C_i(h)\rho_i \tag{7-14}$$

$$\sum_{i=1}^{n} C_i(h) = 1 \qquad \text{for all } h \tag{7-15}$$

$$C_i^{\,f} = \int_0^1 C_i(h)\,dh \qquad \text{for all } i \tag{7-16}$$

7.1.1 Stratification of a two-component system

The set of differential equations (7.13) can be solved easily in closed form when the bed consists of only two components.
Formal integral of equation (7.13) gives

$$C_i(h) = C_i(0)\exp\left(-\alpha\rho_i h + \alpha\int_0^h \bar{\rho}(y)\,dy\right) \qquad \text{for i = 1 and 2} \tag{7-17}$$

The average density of particles at level *h* in the bed for the two-component system is

$$\bar{\rho} = \frac{\rho_1 C_1(h) + \rho_2 C_2(h)}{C_1(h) + C_2(h)} \tag{7-18}$$

The boundary condition $C_i(0)$ represents the concentration of particles of type *i* at the base of the bed. This is an unknown and must be calculated for each species but the solution must satisfy the two conditions (7.15) and (7.16).
Equation (5) requires

$$C_1(0) + C_2(0) = 1 \tag{7-19}$$

at every level in the bed.
The vertical density profile $\bar{\rho}(h)$ is also unknown so that equation (7.17) cannot be used in isolation to calculate the vertical concentration profile of the different particle types. However, the ratio of the concentrations of the two species in a two-component system is independent of $\bar{\rho}(h)$.

$$\frac{C_1(h)}{C_2(h)} = \frac{C_1(h)}{1 - C_1(h)} = \frac{C_1(0)}{C_2(0)}\exp[-\alpha(\rho_1 - \rho_2)h] \tag{7-20}$$

from which

$$C_1(h) = \frac{\frac{C_1(0)}{C_2(0)}\exp[-\alpha(\rho_1 - \rho_2)h]}{1 + \frac{C_1(0)}{C_2(0)}\exp[-\alpha(\rho_1 - \rho_2)h]} \tag{7-21}$$

Equation (7.21) gives the vertical concentration profile of species 1 as a function of the ratio $C_1(0)/C_2(0)$ at the bottom of the bed. This ratio is fixed by the composition of the material that is fed to the jig bed and can be evaluated from equation 7.16

$$C_1^f = \int_0^1 C_1(h)\,dh \tag{7-22}$$

Integration of equation (7.22) using equation (7.21) and solution for $C_1(0)/C_2(0)$ gives

$$\frac{C_1(0)}{C_2(0)} = \frac{1 - \exp[-\alpha(\rho_1 - \rho_2)C_1^f]}{\exp[-\alpha(\rho_2 - \rho_1)C_2^f] - 1}\exp[\alpha(\rho_1 - \rho_2)] \tag{7-23}$$

which is easy to evaluate when the composition of the feed is known. Substitution of this ratio into equation (7.21) gives the vertical concentration profile. Typical concentration profiles are shown in Figure 7.3.

The grade and recovery in the two product streams can be calculated once the equilibrium stratification profiles have been calculated. The yield of total solids to the heavier fraction can be obtained by integrating the concentration profile.

Equipment that is designed to induce stratification of the particles and then to separate them always has a mechanism that enables the stratified bed to be split at some horizontal position. The top layers of the bed contain the lighter particles and the lower layers will include the heavier particles.

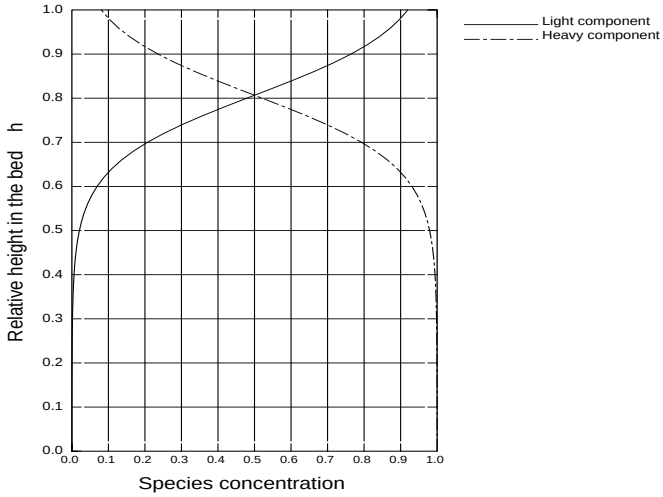

Figure 7-2 *Calculated equilibrium stratification profiles for a binary mixture having components with densities 2670 and 3300 kg/m^3 and initial concentration 0.2 of the lighter component.*

The mass yield of solids in the lighter product obtained by slicing the bed at a relative height h_s is given by

$$Y(h_s) = \frac{\int_{h_s}^{1} \bar{\rho}(h)dh}{\int_{0}^{1} \bar{\rho}(h)dh} \tag{7-24}$$

The recovery of the ith density component to the lighter product at a height h_s is given by

$$R_i(h_s) = \frac{\int_{h_s}^{1} C_i(h)dh}{\int_{0}^{1} C_i(h)dh} = \frac{\int_{h_s}^{1} C_i(h)\,dh}{C_i^f} \tag{7-25}$$

The concentration of component *i* in the lighter product is given by

$$C_i^P = \frac{C_i^f R_i(h_s)}{\sum_i C_i^f R_i(h_s)} \tag{7-26}$$

Equations (7.24), (7.25) and (7.26) can be used to generate grade - recovery and recovery - yield curves using the relative splitting height, h_s as the operating variable.

7.1.2 Stratification in Multicomponent Beds

When the material to be processed contains more than two particle types, the convenient analytical solution given in the previous section is no longer available and a numerical technique must be used to solve the system of differential equations 7.13 Subject to the conditions 7.14 to 7.16.

One obvious approach to the solution of the system of equations (7.13) is to assume a set of $C_i(0)$, integrate Equations (7.13) numerically and check the resulting profiles against equation (7.16). Using an optimization procedure, the initial guesses of $C_i(0)$ can be refined and the procedure repeated. This procedure, however, converges only slowly and exhibits weak stability characteristics.

A much more efficient procedure for integrating the equilibrium equations can be developed using the following method.

Integration of the stratification equations (7.13) from the bottom of the bed with the unknown initial condition $C_i(0) = C_i^0$ gives

$$C_i(h) = C_i^0 \exp[-\alpha\rho_i h + \alpha \int_0^h \bar{\rho}(u)du] \qquad i = 1,2,3....n \tag{7-27}$$

Substituting equation (7.27) into equation (7.16)

$$\int_0^1 C_i^0 \exp[-\alpha\rho_i h + \alpha \int_0^h \bar{\rho}(u)\,du]dh = C_i^f \qquad (7\text{-}28)$$

and rearranging gives an estimate of the concentration of each species at the bottom of the bed

$$C_i^o = \frac{C_i^f}{\int_0^1 \exp[-\alpha\rho_i h + \alpha \int_0^h \bar{\rho}(u)\,du]\,dh} \qquad (7\text{-}29)$$

An iterative method is started by guessing an initial average density profile $\bar{\rho}(h)$ and applying equation (7.29) to calculate C_i^0 for each particle type.

Accumulation of numerical errors *i* prevented by normalizing the $C_i(0)$ to make

$$\sum_i C_i(0) = 1 \qquad (7\text{-}30)$$

at this stage in the calculation.

These initial values $C_i(0)$ can be used in equation (7.27) to get an estimate of the concentration profiles $C_i(h)$ for each particle type and then a new average density profile can be calculated using equation (7.14) The procedure is repeated and continued until the calculated average density profile no longer changes from one iteration to the next.

This iterative procedure is efficient and robust and is capable of generating solutions rapidly for any number of components encountered in practice. The ideal Meyer profile has been found to provide a good starting point and this is easy to calculate.

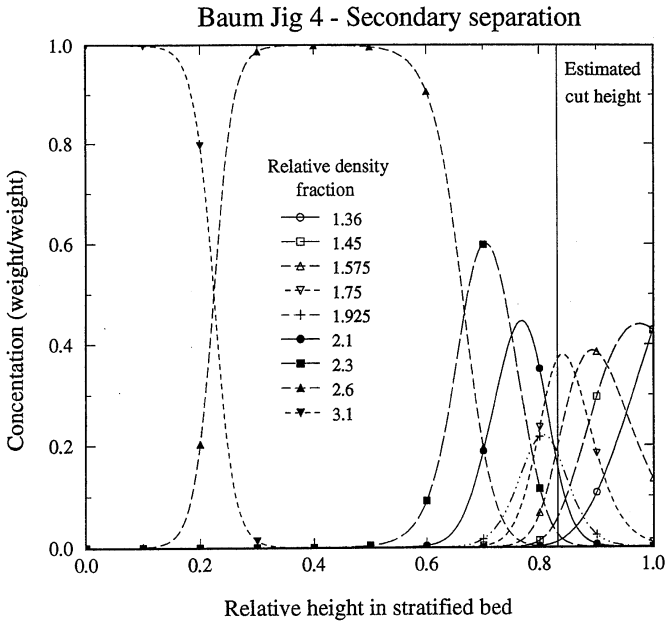

Figure 7-3 *Calculated stratification profiles for nine washability fractions of coal in a industrial Baum jig.*

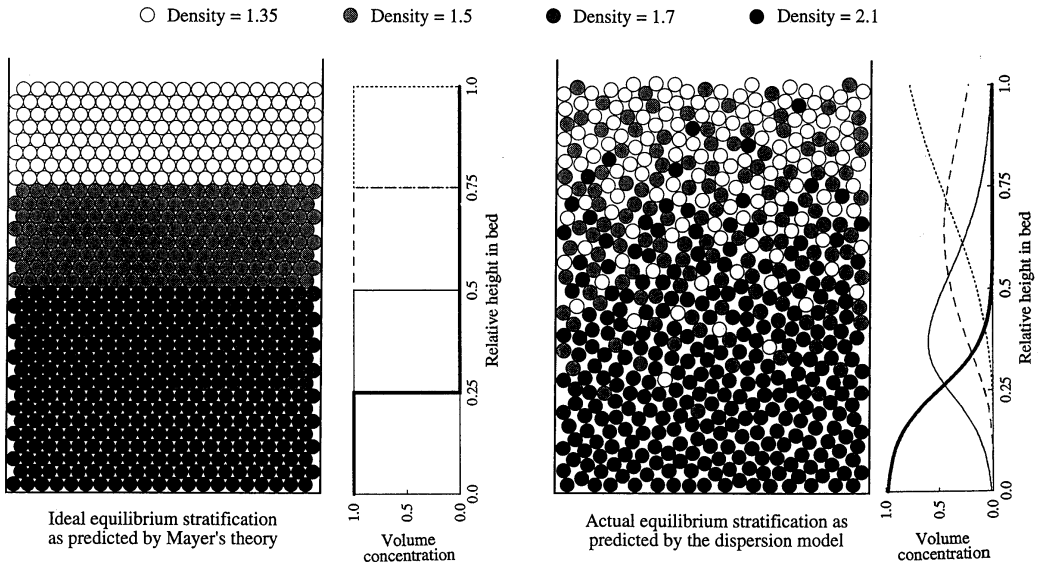

Figure 7-4 *The effect of dispersion on the equilibrium stratification profile in a multicomponent mixture. The beds shown represent accurate simulations using the ideal Mayer theory and the dispersion model. The calculated vertical concentration profiles are also shown. A value of α = 0.03 was used to simulate the dispersed bed.*

The solution for a hypothetical four-component mixture is illustrated in Figure 7.4 which shows a typical equilibrium stratification profile and compares it to the ideal Mayer profile that would be achieved without dispersion.

Specific stratification constant values range from zero for a perfectly mixed bed with no stratification to infinity for perfect stratification. Typical practical values of alpha range from 0.001 m^3/kg for a poor separation to 0.5 m^3/kg for an exceedingly accurate separation. Although independent of the washability distribution of the feed, the specific stratification constant is dependent on the size and shape of the particles and on the type of equipment and its operating conditions. Experience has shown that this method is rapidly convergent over a wide range of conditions. As an example the calculated concentration profiles of 9 washability fractions of coal in an industrial Baum jig are shown in Figure 7.3 .

7.1.3 Performance of continuously operating single- and double-stage jigs.

The mineral jig is designed specifically to stratify a bed of solid particles and a number of different designs have evolved over the years. These all have a common basic operating principle so that it is feasible to build a generic model that can be used to simulate the operation of any continuous jig. Three distinct subprocesses can be identified in a continuous jig: bed stratification produced by the vertical pulsation of the bed, longitudinal transport of the bed due to water flow along the axis of the

jig and splitting of the bed into concentrate and tailing layers.
The water velocity in the longitudinal direction is not uniform and vertical velocity profile exists in the continuous jig. In each compartment of the jig the various bed layers move at different velocities, with the upper layers generally moving faster than the lower ones. The velocities of particles at the end of the bed depend primarily on the velocities of the layers to which they report. The velocity profile at the discharge end of the bed determines the discharge rate of each layer as it leaves the jig. In a continuous jig the overall material balance must be satisfied for each component and the integral condition equation (7.16) must reflect the velocity profile and is replaced by

$$C_\rho^{\,f} = \frac{\int_0^1 C_\rho(h)V(h)\,dh}{\int_0^\infty \int_0^1 C_\rho(h)V(h)\,dh\,d\rho} \qquad (7\text{-}31)$$

where *V(h)* is the longitudinal velocity of the bed at height *h*.

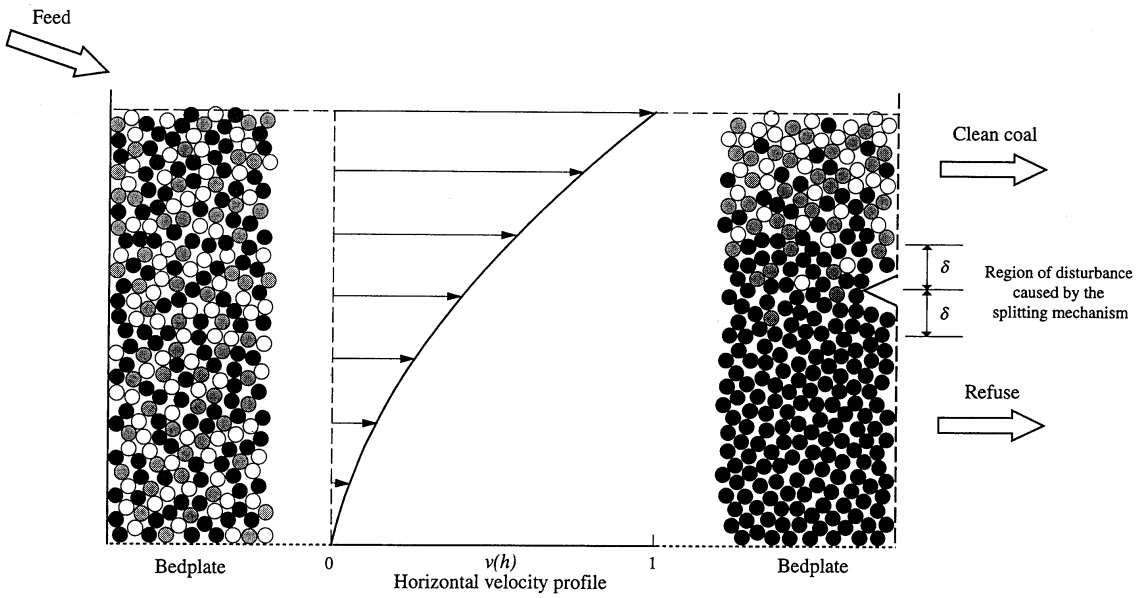

Figure 7-5 *Development of the stratification profile in a continuous jig. The stratified bed is split at the right hand end as shown.*

The velocity profile must be known in order to integrate Equation (7.31). The actual longitudinal velocity at each bed height can only be determined by experiment for any particular equipment type and it will depend on the operating conditions in the unit. Defining a dimensionless velocity by $v(h) = \frac{V(h)}{V_{max}}$ and discretizing Equation (7.31) we get

$$C_i^f = \frac{\int_0^1 C_i(h)v(h)dh}{\sum_{j=1}^{n} \int_0^1 C_j(h)v(h)dh} \tag{7-32}$$

The continuous jigging model for monosize feeds consists of equations (7.13) subjected to the integral conditions given in equations (7.14) and (7.32). Let the denominator of Equation (7.32) be equal to a constant, say *1/β*, then

$$C_i^f = \beta \int_0^1 C_i(h)v(h)\,dh \tag{7-33}$$

A similar iterative solution procedure to the one described in section 7.1.1 is used to model equipment with a significant velocity profile. Substituting equation (7.32) into equation (7.27) and rearranging,

$$\beta C_i^0 = \frac{C_i^f}{\int_0^1 \exp[-\alpha\rho_i h + \alpha \int_0^h \bar{\rho}(u)\,du]\, v(h)\,dh} \tag{7-34}$$

βC_i^o is determined iteratively as before and C_i^o is obtained from

$$C_i^o = \frac{\beta C_i^o}{\sum_{j=1}^{n} \beta C_j^o} \tag{7-35}$$

In the jigging process, particularly for well operated jigs, the longitudinal velocity is expected to increase monotonically from the bottom to the top of the bed. The limited amount of direct measurements of velocity profiles found in the literature, however, does not allow the development of precise models for the velocity profile. A simple but effective empirical model for the velocity profile which does not appear to conflict with the available experimental data is used here and is given by

$$v(h) = \kappa h + (1-\kappa)h^2 \tag{7-36}$$

where κ is a parameter of the model.

In a continuous jig, the separation of stratified layers is affected by refuse and middlings discharge mechanisms. Additional misplacement of clean coal and refuse is believed to happen as a result of the turbulence produced by the operation of these removal systems. The absence of any quantitative experimental work on this effect and the wide variety of refuse ejectors encountered in practice does not allow the precise modeling of this subprocess at present. A simple model which considers that the turbulence produced by splitting the stratified layers creates a perfectly mixed region of relative thickness *2δ* is proposed tentatively here. The yield of solids to the lighter product can now be

calculated by

$$Y(h_s,\delta) = \frac{\frac{1}{2}\int_{h_s-\delta}^{h_s+\delta} \bar{\rho}(h)v(h)dh + \int_{h_s+\delta}^{1} \bar{\rho}(h)v(h)dh}{\int_{0}^{1} \bar{\rho}(h)v(h)dh} \tag{7-37}$$

The recovery of the *i*th density component to the lighter product is given by

$$R_i(h_s,\delta) = \frac{\frac{1}{2}\int_{h_s-\delta}^{h_s+\delta} C_i(h)v(h)dh + \int_{h_s+\delta}^{1} C_i(h)v(h)dh}{\int_{0}^{1} C_i(h)v(h)dh} \tag{7-38}$$

The density distribution of the lighter product by volume is given by

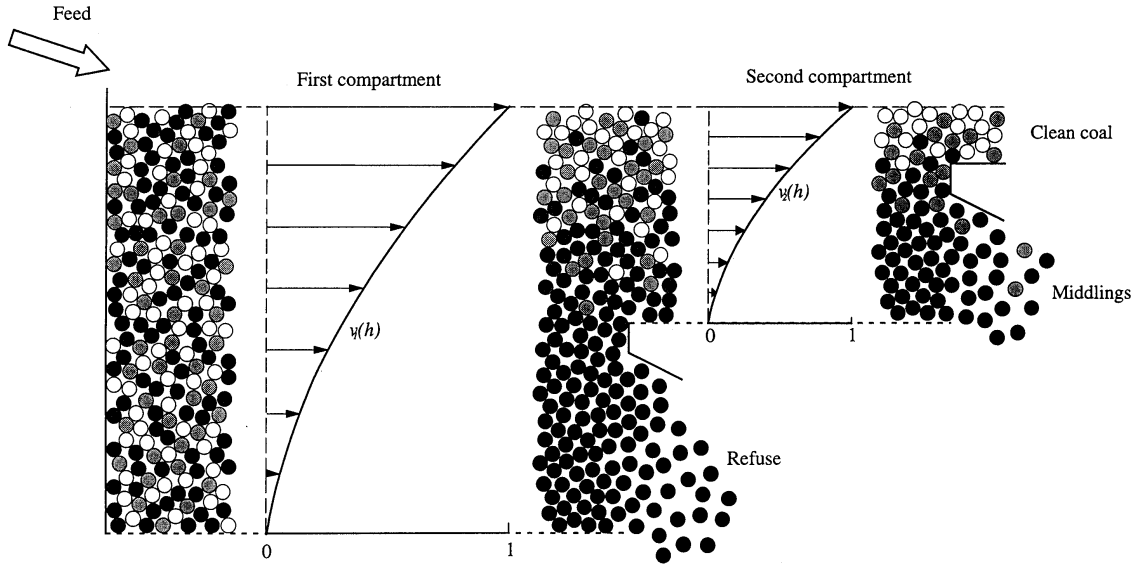

Figure 7-6 *Stratification profiles in a continuous two-stage jig.*

$$C_i^p(h_s,\delta) = \frac{C_i^f R_i(h_s,\delta)}{\sum_{j=1}^{n} C_j^f R_j(h_s,\delta)} \tag{7-39}$$

The effect of the velocity profile can be seen by comparing the simulated beds in Figures 7.4 and 7.5. In each case the same hypothetical four-component mixture was used to simulate the stratified beds. A thick layer of refuse accumulates in the bottom of the moving bed as a result of the longer residence times experienced by the heavier material in the jig. The concentration of the separate components in the lighter product stream is governed by Equation (7.39) and differs significantly

from the equilibrium concentration in the bed itself.

This model can also be used for simulating separations in multiple compartment jigs. The first compartment is modeled as a single compartment jig and the second compartment is considered to be a single compartment with the feed equal to the light product from the first compartment. This is illustrated schematically in Figure 7.6. Thus equation (7.32) becomes

$$C_i^p = \frac{\int_0^1 C_i^{(2)}(h)\, v_2(h)\, dh}{\sum_{j=1}^{n} \int_0^1 C_j^{(2)}(h)\, v_2(h)\, dh} \qquad (7\text{-}40)$$

where C_i^p is the density distribution in the light product from the first compartment and $C_i^c(h)$ and $v_2(h)$ are the equilibrium concentration and velocity profiles in the second compartment, respectively.

The same computational procedure can be used for the second stage as was used for the first stage.

Table 5.1 Application of the Multicomponent Continuous Model to the Operation of Industrial Jigs

Jig	Size (mm)	Stage	Measured yield (%)	Estimated value of α	Calculated cut height h_s	Calculated bed density at the cutter position $\bar{\rho}(h_s)$
Baum 1	150 x 1.4	Primary	30.6	0.027	0.56	1.78
		Secondary	13.1	0.091	0.39	1.56
Baum 2	100 x 1.4	Primary	44.5	0.046	0.65	1.45
Baum 3	50 x 1	Primary	20.6	0.009	0.49	2.10
		Secondary	30.1	0.028	0.56	1.95
Baum 4	50 x 0.6	Primary	5.0	0.006	0.27	2.56
		Secondary	71.7	0.114	0.83	1.77
Batac 1	12 x 0.6	Primary	7.4	0.019	0.30	3.40
		Secondary	96.4	0.113	0.98	1.68
Batac 2	19 x 0.6	Primary	14.8	0.028	0.39	2.23
		Secondary	17.3	0.072	0.42	1.66
Batac 3	50 x 0.6	Primary	15.2	0.068	0.42	1.70

The data in Table 5.1 show that the value of α varies between the first and second stages of all the industrial jigs that have been analyzed. The most probable reason for this is the fact that the bed does not usually achieve equilibrium stratification profile in the first stage because of insufficient residence time. This shows up as an apparently low value of α. Since the solids entering the second stage are already partially stratified, it is easier to reach the equilibrium stratification profile in the limited residence time that is available.

Any complex jig can be modeled by an appropriate combination of the stratification model with models of the material transport and bed splitting phenomena that take place in the equipment. This versatile stratification model can be used to describe the behavior of other autogenous gravity separation devices such as the pinched sluice and the Reichert cone.

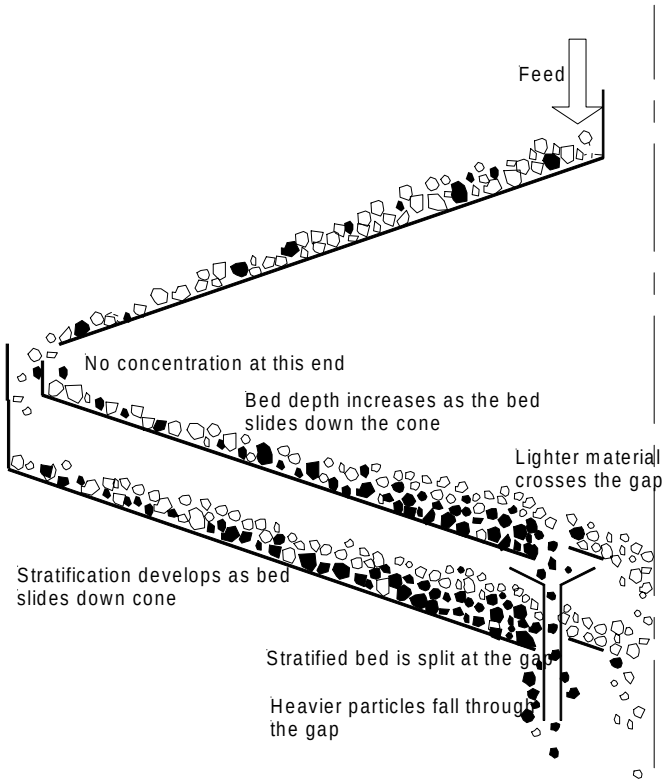

Figure 7-7 *Details of the concentrating action of the Reichert cone. A double cone is illustrated.*

7.1.4 A Model for the Pinched Sluice and the Reichert Cone

The pinched sluice and the Reichert cone are two simple devices that rely on stratification to effect a separation of particles of different densities. Unlike the jig, these devices rely on a natural phenomenon to induce stratification rather than the purposeful jigging action of the jig.

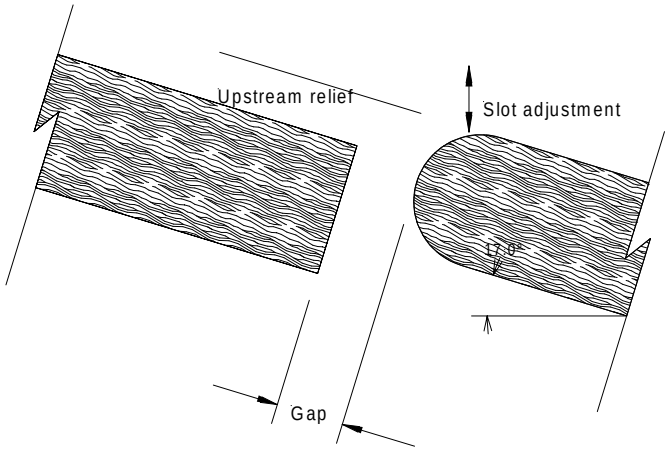

Figure 7-8 *Details of the gap at the lower end of the cone. The vertical position of the bullnose is determined by the slot setting.*

The principles that govern the concentrating action of the pinched sluice and the Reichert cone are comparatively straight forward. The bed of particles is washed down the inside surface of the inverted cone as a sliding bed. The turbulence in the flowing stream induces stratification in the sliding bed of particles with the heavy particles tending to move towards the floor of the sliding bed. At the bottom of the cone, a slit in the floor of the cone allows the lower layers of particles the bed to be discharged while

the upper layers pass over the gap. The details of the cone arrangement are shown in Figure 7.7 Because of the steadily decreasing area available for flow as the particle bed slides down the cone, the thickness of the bed increases significantly toward the apex of the cone. This thickening of the bed promotes the stratification of the particles because the lighter particles migrate upward through the particle layers more readily and more quickly than the heavier particles.

The fraction of the bed that is recovered through the slots is controlled by variation of the upstream relief at the slot as shown in Figure 7.8. The slot insert can be adjusted at 9 vertical positions from the highest to the lowest. The higher the upstream relief the greater the proportion of the particle bed that is recovered to the concentrate.

Two well-documented experimental studies on the behavior of the Reichert provide some excellent data from which the essential nature of the operation of the Reichert cone can be established and a useful predictive model can be developed. Schematics of the four standard Reichert cone modules are shown in Figure 7.9 . A basic cone module can consist of a single separating cone or the flow can be split on to 2 cone surfaces as shown in Figure 7.9 Which allows the cone to handle a greater feed. Two multiple cone modules are common: the DSV module which consists of a double cone followed by a single cone with a variable gap, and the DSVSV module which has an extra single cone with variable gap to clean the concentrate further. The two cleaning stages of the DSVSV module makes this configuration more suitable for cleaning duties while the DSV module is better suited to roughing and scavenging. Actual cone units that are

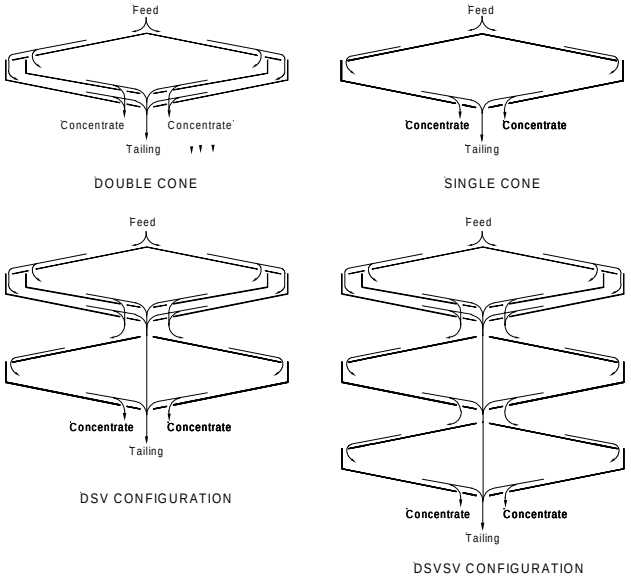

Figure 7-9 *The four basic cone modules from which operating Reichert cone stacks are assembled.*

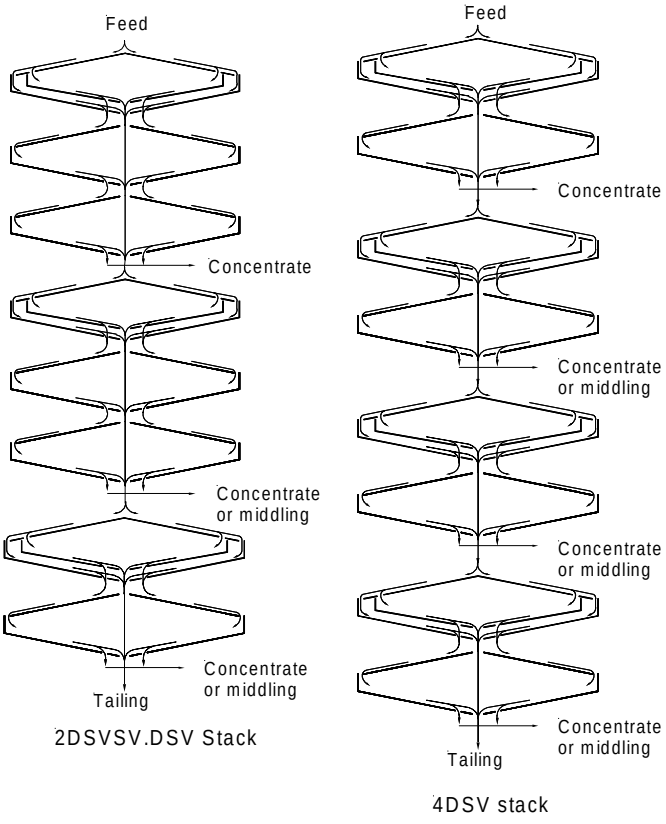

Figure 7-10 *2dSVSV.dSV and 4DSV Reichert cone stacks that are commonly used for cleaning and roughing duties respectively.*

used in industrial practice are assembled as stacks of these standard modules. Two common unit stacks are shown in Figure 7.10. Nine stack configurations are commonly used in practice and these are SV, DSV, 2DSV, 3DSV, 4DSV, DSVSV, 2DSVSV, 3DSVSV and 2DSVSV.DSV with the symbols having the following meaning: D = double cone with fixed gap, SV = single cone with variable gap. The numerical prefix indicates the multiple of basic configuration that is repeated in the stack. The internal flow pattern for the heavies and the lights in the stack is fixed on installation and would not normally be altered afterwards. The normal internal flow arrangement of the 4DSV and 2DSVSV.DSV configurations is shown in Figure 7.10.

The variation of the concentrate flow with the feedrate to the cone surface for three different slot settings is shown in Figure 7.11. The data from the investigations cited above for a variety of ores are remarkably consistent and show clearly the effects of both feedrate and slot settings.
There are two phenomena that occur on the cone surface that must be modeled in order to simulate the operating performance of a simple cone: the stratification profile that develops in the sliding bed during its passage down the cone surface, and the splitting action of the bullnose splitter at the gap. The split that is achieved is determined primarily by the vertical position of the bullnose splitter as shown in Figure 7.8. The standard cone provides 9 pre-specified slot positions to control the bullnose. Slot 1 corresponds to maximum and slot 9 to minimum cut at the gap. Once the slot position has been chosen, the amount of solid taken off by the gap is a function of the total solids rate that flows down the cone surface.

Good experimental data are available to model the effects of both total solid flow and slot position on the underflow through the slot. The data for slot positions 1,5 and 9 are shown in Figure 7.11. The data for other slot positions can easily be obtained by interpolation of the data in Figure 7.11. Obviously the amount flowing through the gap cannot exceed the total flow on the cone and the data have a distinct break at the point of intersection with the line *underflow = total flow* which is a straight line of slope 1 through the origin as shown in the Figure 7.11. Each slot setting has a critical feedrate which must be exceeded to ensure that at least some material clears the concentarte gap and reports to tailings. When the feed rate falls below the critical flow, all the solid exits through the gap and no concentration is achieved. This effect is built into the cone model in MODSIM to ensure that this underloaded condition, if it occurs in the plant, is properly simulated. The pattern of behavior shown in Figure 7.11 has been confirmed by extensive tests on other ore types. (See Holland-Batt, 1978, Figure 13). The linear relationship between concentrate flow and the total flow on the cone is not surprising. The more material that is presented to the splitter the greater the flow through the gap. The point of convergence, POC in

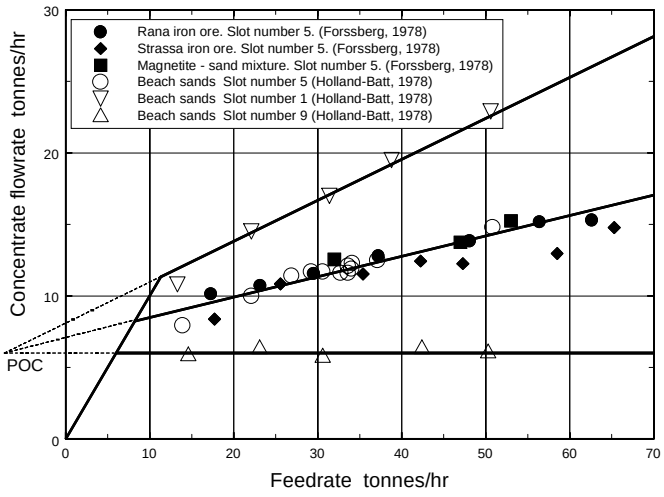

Figure 7-11 *Concentrate take off rate as a function of the feed rate to the cone and the variable slot setting. This data obtained on a single isolated cone.*

Figure 7.11, and the slopes of the lines vary with ore type and Table 1 summarizes the data that are available. These variations are probably associated primarily with the shape of the particles but this effect has never been investigated.

In order to calculate the composition of the two discharge streams from the cone, it is necessary to model the stratification of the solid particles that occurs during the passage of the sliding bed down the cone surface. Stratification is a complex process, but a good realistic quantitative description of this phenomenon on the cone is provided by the equilibrium profile that balances the potential energy decrease that occurs with stratification against the random particle motions in the sliding bed. This model of stratification is described in section 7.1.1 and has been found to provide an excellent

Table 5.2 Parameters that define the flow split at the gap of a single cone.

Ore type	Coordinates of POC	Slope of the line	Reference
Beach sands	(-7.3, 6.0)	0.0359×(9 - slot #)	Holland-Batt, 1978
Iron ore and magnetite-sand mixtures	(-31.0, 2.5)	0.0359×(9 - slot #)	Forssberg, 1978, Forssberg & Sandström, 1981
Witwatersrand quartzite	(0.0, 3.5)	0.055×(9 - slot #)	Holland-Batt, 1978

description of the operating behavior of Reichert cones. Figure (7.12) shows experimental data obtained with iron ore on a single Reichert cone. The stratification model is seen to describe the behavior of the cone well. The experimental data points were obtained at different slot settings, varying feed flowrates and solid content in the feed. The model predictions were made using the binary stratification model wit a specific stratification constant of 0.0008 m^3/kg. This model is complex and highly nonlinear since it allows for the obvious fact that the stratification of the bed is governed by the makeup of the feed material. The model is computationally intensive since it requires the solution of a set of coupled differential equations — one for each type of particle — with integral boundary conditions. Once the behavior of a single cone can be modeled, the behavior of an entire cone stack can be synthesized by combining the models for the single cones appropriately. The double cone is synthesized as two single cones in parallel, each one receiving one half of the feed to the stage.

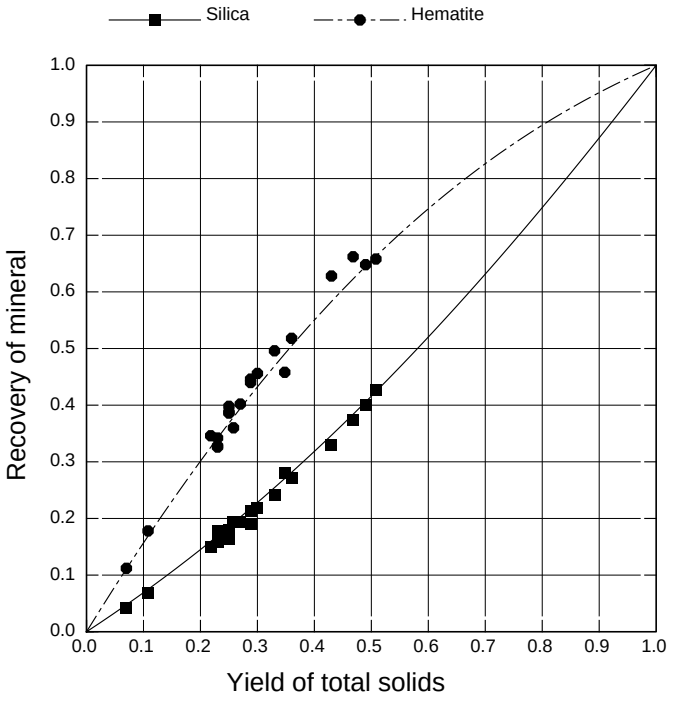

Figure 7-12 *Comparison between the stratification model and the experimental performance of a single stage Reichert cone*

The calculation of the performance of a single module and a composite cone stack

proceeds as follows.
TECHNICAL NOTES 1.Calculate the composition (distribution of particle size and particle composition) of the feed to the stage. This may be the gap underflow from the previous stage or it may be the combined concentrates and/or rejects from several stages higher up in the cone stack or from other units in the plant or it may be the plant feed itself.
TECHNICAL NOTES 2.Use the stratification model to calculate the equilibrium stratification profile of the sliding bed at the gap using the feed from step 1 as the model input.
TECHNICAL NOTES 3.Calculate the gap take off flowrate from the flow model described by Figure 7.11 and Table 5.2
TECHNICAL NOTES 4.Split the calculated stratified bed at the horizontal level that will give the correct gap takeoff established in step 3.
TECHNICAL NOTES 5.Integrate the stratified bed from the floor to the splitting level and from the splitting level to the top of the bed to calculate the composition of the concentrate and discard streams.
TECHNICAL NOTES 6.Use these streams to constitute the feeds to the lower cones on the stack and repeat steps 1 - 5 as necessary.
TECHNICAL NOTES 7.Combine all the concentrates and discards from the cone stack appropriately to constitute the concentrate, middlings, and tailings from the unit.
The composition of the concentrate stream is established by the stratification that occurs while the bed of solids is sliding down the inside surface of the separating cone. Provided that the residence time on the cone is sufficiently long to allow the equilibrium stratification pattern to be established, the composition of the concentrate stream can be calculated using the equilibrium stratification profile as described in section 5.1.4.
It is comparatively straightforward to apply the model developed above to each stage in a stack and then to combine the concentrate streams appropriately to model the entire cone unit. This is the approach taken in MODSIM which allows any of the standard configurations to be specified.
Although each individual cone in the stack produces only a concentrate and tailings stream, the cone stack as a whole can be configured to produce a concentrate, a tailing and, if required, a middling. A middling stream can be constituted from the concentrate streams produced by the lower cones in the stack as shown in Figure 7.10. If a middling stream is produced, it is usually returned to the feed of the stack.
The value of α that is achieve on a Reichert cone is significantly lower than that achieve in a jig. The stratification action of the cone is simply not as efficient as in the jig. The experimental data that is available indicates that the value of α should be about 0.002 on the cone.

1. Bibliography

(Holland-Batt A.B. Design of gravity concentration circuits by use of empirical mathematical models. Proc. 11th Commonwealth Mining and Metallurgical Congress, Institution of Mining and Metallurgy, 1978. Forssberg E. and Sandstrom E. Utilization of the Reichert cone concentrator in ore processing. Industrie Mmineral - Mineralurgie, Nov. 1979 pp. 223-243. Forssberg E and Sandstrom E. Operational characteristics of the Reichert cone in ore processing. Proc. 13th International Mineral Processing Congress, Warsaw 1979. J. Laskowski, Editor Elsevier Scientific Publishing Co. 1981. Vol II pp. 1424-1481.